The role of the Coriolis interaction on vector correlations in molecular predissociation: Excitation of isolated rotational lines

Vladislav V. Kuznetsov,[1] Peter S. Shternin,[2] and Oleg S. Vasyutinskii[2,a)]
[1]*Space University of Aerospace Instrumentation, 190000 Saint-Petersburg, Russia*
[2]*Ioffe Physico-Technical Institute, Russian Academy of Sciences, 194021 Saint-Petersburg, Russia*

(Received 16 January 2009; accepted 5 March 2009; published online 6 April 2009)

We present the full quantum mechanical expressions for the polarization differential cross sections of the photofragments produced in slow predissociation of a parent molecule via isolated rotational branches. Both radial and Coriolis nonadiabatic interactions between the molecular potential energy surfaces have been taken into account. The expressions describe the recoil angle distribution of the photofragments and the distributions of the photofragment angular momentum polarization (orientation and alignment) in terms of the anisotropy parameters of the ranks $K=0,1,2$. The explicit expressions for the anisotropy parameters are presented and analyzed which contain contributions from different possible photolysis mechanisms including incoherent, or coherent optical excitation of the parent molecule followed by the radial, or Coriolis nonadiabatic transitions to the dissociative states. The obtained expression for the zeroth-rank anisotropy parameter β is valid for any molecule and for an arbitrary value of the molecular total angular momentum J. The expressions for the orientation $(K=1)$ and alignment $(K=2)$ anisotropy parameters are given in the high-J limit in terms of the generalized dynamical functions which were analyzed for the case of photolysis of linear/diatomic molecules. As shown, the Coriolis nonadiabatic interaction results in several new photolysis mechanisms which can play an important role in the predissociation dynamics. © *2009 American Institute of Physics*. [DOI: 10.1063/1.3106402]

I. INTRODUCTION

Recently we have developed full quantum mechanical expressions describing the recoil angle dependence of the spin and orbital orientation and alignment of the fragments produced in one-photon molecular photodissociation beyond the axial recoil approximation.[1–3] The parent molecules were assumed to be isotropically distributed in space.

An important result of this theory is that within the first-order time-dependent perturbation theory the recoil angle dependence of the angular momentum polarization of the photofragments with the angular momentum j_A can be presented in the same universal form for any photodissociation process in a diatomic or polyatomic molecule. The expressions can be written in terms of the anisotropy parameters β, α_K, s_K, γ_K, γ'_K, and η_K of the ranks $K=0,\ldots,2j_A$ or, alternatively, in terms of the anisotropy transforming coefficients $\mathbf{c}^K_{k_d q_k}$, where $k_d=0,1,2$ and $q_k=-\min(K,k_d)\ldots\min(K,k_d)$ are the rank of the photolysis photon and its projection onto the *recoil direction*, respectively.[3]

The particular expressions for the anisotropy parameters/anisotropy transforming coefficients indeed depend on the photodissociation mechanism (direct dissociation, predissociation, etc.) and on the symmetry of the parent molecules (linear, bent, etc.). In case of direct photodissociation of linear/diatomic molecules, the theory provides analytical quasiclassical expressions for the anisotropy parameters.[1] In case of slow predissociation, the theory provides full quantum mechanical expressions for the anisotropy parameters in the high-J limit.[2]

Two groups of nonadiabatic interactions between different reactive potential energy surfaces (PESs) can be important in the predissociation of a linear molecule: the homogeneous (radial) interaction and the inhomogeneous (Coriolis) interaction.[4,5] The former interaction preserves the quantum number Ω, the projection of the molecular total angular momentum J onto the internuclear axis, while the latter interaction changes the projection Ω. The spin-orbit interaction preserves the projection Ω and, therefore, belongs to the former group.

Slow predissociation when the molecule lives much longer than the rotational period has been discussed in our previous paper[2] where we assumed that only the radial nonadiabatic interactions occur. Slow predissociation in the presence of the Coriolis interactions has been discussed in our paper[3] for the case of the broadband excitation of the P, Q, and R rotational branches; however, the more usual (and likely more useful for experimentalist) case when the different rotational branches are resolved has been dropped out in that study.

The main aim of the present paper is to derive and discuss the recoil angle dependence of the angular momentum polarization of the fragments produced in slow predissociation mediated by the radial and Coriolis nonadiabatic interactions under the condition when all individual molecular J states are resolved. The derivation has been carried out in the

a)Electronic mail: osv@pms.ioffe.ru.

line of our previous papers[1–3] where the adiabatic basis set of the diatomic molecule wave functions was used.

General expressions for the angular momentum distribution of photofragment state multipole moments (polarization differential cross sections) produced in molecular photodissociation are presented in Sec. II in the case of arbitrary J values and in the case of the high-J limit.

These expressions were transformed to the case of slow predissociation and then analyzed in detail in Sec. III for several most important values of the polarization cross section rank $K=0$, 1, and 2. The angular distribution of the molecular photofragments ($K=0$) for arbitrary values of the total angular momentum J is considered in Sec. III A. The angular momentum distributions of the photofragment state multipoles of the ranks $K=1$ (orientation) and $K=2$ (alignment) are derived and analyzed in detail in the high-J limit in Secs. III B and III C, respectively. The obtained expressions for the corresponding anisotropy parameters contain the contributions from all possible photolysis mechanisms.

II. GENERAL EXPRESSION FOR THE PHOTOFRAGMENT ANGULAR MOMENTUM DISTRIBUTION IN MOLECULAR PREDISSOCIATION

The general expression for the recoil angle distribution of the angular momentum polarization of the photofragments produced in molecular photodissociation has been derived by Kuznetsov and Vasyutinskii[1] and by Shternin and Vasyutinskii[3] from the scattering wave function formalism using the parity unadapted and parity adapted representations of the total molecular wave function, respectively. As shown in Ref. 3 (see also discussion in Ref. 2), these two distributions are equivalent to each other because the expansion of the total excited state scattering function can be done using any appropriate orthogonal set of the wave functions which depends on the recoil direction $\hat{\mathbf{k}}$, incoming vector $\mathbf{R}/R$, and all electronic coordinates of the molecule. Therefore, the choice of a particular orthogonal set is mostly determined by the convenience of its practical use.

The general expression for the recoil angle distribution of the photofragment angular momenta polarization in molecular photodissociation can be presented in the form of expansion over the product of the two D-functions:[3]

$$\sigma_{KQ}^{(j_A)}(\hat{\mathbf{k}}) = \frac{\sigma_0}{4\pi} \sum_{k_d,q_d} \sum_{q_k} \mathbf{c}_{k_d q_k}^{K} D_{Qq_k}^{K^*}(\phi,\theta,0) D_{q_d q_k}^{k_d}(\phi,\theta,0) E_{k_d q_d}(\mathbf{e}), \tag{1}$$

where $D_{q_d q_k}^{k_d}(\phi,\theta,0)$ is a Wigner D-function,[6] ϕ and θ are polar angles specifying the recoil direction $\hat{\mathbf{k}}$, and $\sigma_0 = \langle \sigma_{00}^{(j_A)} \rangle$ is the total photodissociation cross section, where the angular brackets indicate integration over all recoil directions.

The $\sigma_{KQ}^{(j_A)}(\hat{\mathbf{k}})$ in Eq. (1) is the polarization differential predissociation cross section describing the photofragment A flying apart in the recoil direction $\hat{\mathbf{k}}$. The rank K and its laboratory frame projection Q describe the orientation and alignment[7] of the fragment angular momentum j_A; $K=0,\ldots,2j_A$ and $Q=-K,\ldots,K$. $E_{k_d q_d}(\mathbf{e})$ is the photon polarization matrix,[8] where $\mathbf{e}$ is the light polarization vector, $k_d=0$, 1, 2 and $q_d=-k_d,\ldots,k_d$ are the photon rank and its laboratory frame projection, respectively.

The *anisotropy transforming coefficients* $\mathbf{c}_{k_d q_k}^{K}$ in Eq. (1) are scalar values which contain all information about the photodissociation dynamics and can be either determined from experiment or calculated from theory:

$$\begin{aligned}
\mathbf{c}_{k_d q_k}^{K} = {} & \frac{3(2K+1)^{1/2}}{(2j_A+1)^{1/2}} \mathcal{N}^{-1} \sum_{\Omega_k,\Omega_k'} \sum_{\Omega_A,\Omega_B} \sum_{\Omega_A'} \sum_{n,n'} \sum_{k_d,q_d,q_k} (\mathcal{T}_{j_A\Omega_A j_B\Omega_B}^{n\Omega_k})^* \mathcal{T}_{j_A\Omega_A' j_B\Omega_B}^{n'\Omega_k'} (-1)^{q_k} [(2k_d+1)]^{1/2} C_{j_A\Omega_A' K-q_k}^{j_A\Omega_A'} \\
& \times \sum_{J,J'} e^{i(\pi/2)(J-J')} (-1)^{J+J_i} \sqrt{2J'+1} \begin{Bmatrix} J' & J & k_d \\ 1 & 1 & J_i \end{Bmatrix} \sum_{q,q'} \sum_{\bar{n},\Omega_R} \sum_{\bar{n}',\Omega_R'} \sum_{J_i,\Omega_i,v_i} C_{J_i\Omega_i 1q}^{J\Omega_R} C_{J_i\Omega_i 1q'}^{J'\Omega_R'} C_{J'\Omega_k' k_d q_k}^{J\Omega_k} W(v_i,J_i) \\
& \times \langle \Psi_{\bar{n},\Omega_R}^{\mathrm{el}} \chi_{\bar{n}\Omega_R;n\Omega_k}^{J}(R) | d_q | \Psi_{\Omega_i}^{\mathrm{el}} \chi_{\Omega_i}^{J_i}(R) \rangle^* \langle \Psi_{\bar{n}',\Omega_R'}^{\mathrm{el}} \chi_{\bar{n}'\Omega_R';n'\Omega_k'}^{J}(R) | d_{q'} | \Psi_{\Omega_i}^{\mathrm{el}} \chi_{\Omega_i}^{J_i}(R) \rangle,
\end{aligned} \tag{2}$$

where $\mathcal{N}$ is the normalization factor:

$$\begin{aligned}
\mathcal{N} = {} & (2j_A+1)^{-1/2} \sum_{J} \sum_{\Omega_k} \sum_{\Omega_A,\Omega_B} \sum_{n,n'} \sum_{q,q'} \sum_{\bar{n},\Omega_R} \sum_{\bar{n}',\Omega_R'} \sum_{J_i,\Omega_i,v_i} (\mathcal{T}_{j_A\Omega_A j_B\Omega_B}^{n\Omega_k})^* \mathcal{T}_{j_A\Omega_A j_B\Omega_B}^{n'\Omega_k} C_{J_i\Omega_i 1q}^{J\Omega_R} C_{J_i\Omega_i 1q'}^{J\Omega_R'} W(v_i,J_i) \\
& \times \langle \Psi_{\bar{n},\Omega_R}^{\mathrm{el}} \chi_{\bar{n}\Omega_R;n\Omega_k}^{J}(R) | d_q | \Psi_{\Omega_i}^{\mathrm{el}} \chi_{\Omega_i}^{J_i}(R) \rangle^* \langle \Psi_{\bar{n}',\Omega_R'}^{\mathrm{el}} \chi_{\bar{n}'\Omega_R';n'\Omega_k}^{J}(R) | d_{q'} | \Psi_{\Omega_i}^{\mathrm{el}} \chi_{\Omega_i}^{J_i}(R) \rangle.
\end{aligned} \tag{3}$$

As can be shown from Eqs. (2) and (3), $\mathbf{c}_{00}^{0}=-\sqrt{3}$. The set of the coefficients $\mathbf{c}_{k_d q_k}^{K}$ is an alternative to the set of the known anisotropy parameters β, α_K, s_K, γ_K, γ_K', and η_K,[9,10] as they are simply proportional to the corresponding anisotropy parameters in pairs. The relationship between the coefficients $\mathbf{c}_{k_d q_k}^{K}$ and the anisotropy parameters has been tabulated by Shternin and Vasyutinskii.[3] Whereas the anisotropy parameters are all real and normalized to the orientation and

alignment of the photofragments averaged over all recoil directions,[9,10] the coefficients $\mathbf{c}^K_{k_d q_k}$ are in general complex and obey the symmetry relation

$$\mathbf{c}^K_{k_d -q_k} = (\mathbf{c}^K_{k_d q_k})^*. \tag{4}$$

The values J_i and J in Eq. (2) are the initial (ground state) and the final (excited state) total molecular angular momenta, respectively. The term $C^{j_A \Omega'_A}_{j_A \Omega_A K - q_k}$ is a Clebsch–Gordan coefficient, and the term in the curly brackets is a $6j$ symbol.[6] The term $W(v_i, J_i)$ describes the population of the rovibrational energy levels of the parent molecules.

The helicity quantum number Ω_i in Eqs. (2) and (3) is a body-frame projection of the angular momentum J_i onto the internuclear axis. The helicity quantum numbers Ω_R and Ω_k are body-frame projections of the excited state angular momentum J onto the internuclear axis $\mathbf{R}$ and the recoil direction $\hat{\mathbf{k}}$, respectively. The angular momenta j_A and j_B are the electronic angular momenta of the fragments A and B, respectively, and Ω_A and Ω_B are the corresponding projections onto the recoil direction. Due to the cylindrical symmetry of the molecule in the long range $\Omega_k = \Omega_A + \Omega_B$.

The terms in the last line of Eq. (2) are transition dipole moments written in the molecular frame. They obey the following selection rule: $\Omega_R = \Omega_i + q$, where the indices q denote the spherical basis[8] for the components of the dipole moment d_q with respect to the molecular frame. The indices q, q' are limited to the values 0 and ± 1, indicating parallel and perpendicular optical transitions, respectively. In the transition dipole matrix elements the functions $\Psi^{\mathrm{el}}_{\bar{n}\Omega_R}$ and $\Psi^{\mathrm{el}}_{\Omega_i}$ denote the electronic adiabatic wave functions of the molecular excited and ground states, respectively, and $\chi^J_{\bar{n}\Omega_R, n\Omega_k}(R)$ and $\chi^{J_i}_{\Omega_i}(R)$ are the corresponding scattering (vibrational) wave functions.[1,2]

The terms $\mathcal{T}^{n\Omega_k}_{j_A \Omega_A j_B \Omega_B}$ in Eq. (2) are the expansion coefficients of the adiabatic molecular electronic states over the fragment basis $|j_A \Omega_A\rangle |j_B \Omega_B\rangle$ in the asymptotic region:[10,11]

$$\Psi^{\mathrm{el}}_{n\Omega_k} \equiv |n\Omega_k\rangle \to \sum_{\Omega_A \Omega_B} \mathcal{T}^{n\Omega_k}_{j_A \Omega_A j_B \Omega_B} |j_A \Omega_A\rangle |j_B \Omega_B\rangle, \quad R \to \infty. \tag{5}$$

The index q_k in Eq. (2) is the *coherent quantum number* which is equal to the projection of the photon rank k_d *and* of the photofragment rank K onto the recoil direction $\hat{\mathbf{k}}$. As recently shown by Shternin and Vasyutinskii,[3] the quantum number q_k is preserved in any photolysis reaction irrespectively of the photolysis mechanism. The physical meaning of this statement can be clarified by presenting the photon polarization matrix in the recoil frame:

$$E_{k_d q_k}(\mathbf{e}) = \sum_{\mu_1 \mu_2} (-1)^{\mu_2} C^{k_d q_k}_{1\mu_1 1 - \mu_2} e_{\mu_1} (e_{\mu_2})^*, \tag{6}$$

where μ_1 and μ_2 are the projections of the photon angular momentum (photon helicities) onto the recoil direction $\hat{\mathbf{k}}$. According to the symmetry of the Clebsch–Gordan coefficient in Eq. (6), the index $q_k = \mu_1 - \mu_2$ can take the values $q_k = 0, \pm 1, \pm 2$ and describes the coherence introduced by the incident photon to the molecular excited states. From the other side, the symmetry of the Clebsch–Gordan coefficient in Eq. (2) implies the relationship $q_k = \Omega_A - \Omega'_A = \Omega_k - \Omega'_k$, where the angular momentum helicities Ω_k and Ω'_k are also defined in the recoil frame. Therefore, the coherence introduced by the absorbed photon to the molecule is preserved during the photolysis and transferred to the residual coherence in the photofragment quantum states.

Equation (2) takes into account both radial and Coriolis nonadiabatic interactions resulting in the transitions between the excited state PESs. The radial nonadiabatic transitions obey the selection rule $\Omega_k = \Omega_R$, while the Coriolis nonadiabatic transitions obey the selection rule $\Omega_k = \Omega_R \pm 1$.[4]

The kinematic (recoil-angle-dependent) part of the photofragment polarization cross section in Eq. (1) has a universal form which can be used for description of any photolysis reaction of a diatomic or polyatomic molecule and is valid for any integer or half-integer J values.[3] The anisotropy transforming coefficients $\mathbf{c}^K_{k_d q_k}$ are presented in Eq. (2) in the form of expansion over the diatomic-like molecular wave functions. Therefore, they can be directly used for analysis of this type of molecules.

The case of slow predissociation when the molecule lives much longer than the rotational period can be readily obtained from the general expression for the anisotropy transforming coefficients in Eq. (2) by holding the condition $J = J'$ because in this case the rotational level J, J' coherence can be neglected.[2] An equivalent angle recoil distribution is also given in Ref. 2.

The terms with $\Omega_R = \Omega'_R$ in Eq. (2) describe incoherent optical excitation, while the terms with $\Omega_R \neq \Omega'_R$ describe coherent optical excitation from a single initial electronic state $|\Omega_i\rangle$. In the case of slow predissociation when an isolated rotational J state is optically excited, the latter terms describe excitation of a single J state which belongs either to two coherently excited electronic states or to a single double degenerate electronic state via the transitions $^1\Sigma \to {}^1\Pi_{\pm 1}$ or $|\Omega_i| = 1/2 \to |\Omega_R| = 1/2$ (e.g., $^2\Sigma_{\pm 1/2} \to {}^2\Pi_{\pm 1/2}$).

In the high-J limit, $(J_i, J \gg 1)$, Eq. (2) can be simplified using the asymptotic expressions for the Clebsch–Gordan coefficients and $6j$ symbols:[6]

$$\begin{aligned}\mathbf{c}^K_{k_d q_k} = {} & 3(2K+1)^{1/2} \mathcal{N}^{-1} \sum_{q,q'} \sum_A (-1)^{k_d + q_k + q'} C^{AQ'}_{1q1-q'} \\ & \times d^A_{Q'0}\left(\frac{\pi}{2}\right) d^{k_d}_{q_k 0}\left(\frac{\pi}{2}\right) C^{A0}_{1k1-k} C^{k_d 0}_{1k1-k} \sum_{\tilde{q},\tilde{q}'} f_K(q,q',\tilde{q},\tilde{q}') \\ & \times \delta_{(\tilde{q}-\tilde{q}'),q_k},\end{aligned} \tag{7}$$

where $d^A_{Q'0}(\pi/2)$ is the Wigner d-function[6] and $k = J - J_i$. The normalization coefficient $\mathcal{N}$ can be expressed in the high-J limit as:

$$\mathcal{N} = \sum_{q,q'} \sum_A (-1)^{k+q'} C^{AQ'}_{1q1-q'} d^A_{Q'0}\left(\frac{\pi}{2}\right) C^{A0}_{1k1-k} \sum_{\tilde{q}} f_0(q,q',\tilde{q},\tilde{q}). \tag{8}$$

According to the symmetry of the Clebsch–Gordan coefficient in Eq. (7), the index Q' is equal to $Q' = q - q'$. The term $f_K(q,q',\tilde{q},\tilde{q}')$ in Eq. (7) is the generalized predissocia-

tion dynamical function which involves the terms describing both the radial and the Coriolis nonadiabatic interactions. It can be written as[1,3]

$$
\begin{aligned}
f_K(q,q',\tilde{q},\tilde{q}') &= \sum_{\Omega_k,\Omega_k'} \sum_{\Omega_R,\Omega_R'} \sum_{n,n'} \sum_{\bar{n},\bar{n}'} \sum_{j_B,\Omega_B} \sum_{\Omega_A,\Omega_A'} \sum_{J_i,v_i,\Omega_i} (\mathcal{T}^{n\Omega_k}_{j_A\Omega_A j_B\Omega_B})^* \\
&\times \mathcal{T}^{n'\Omega_k'}_{j_A\Omega_A' j_B\Omega_B} (-1)^{j_A+K+\Omega_A'} \\
&\times \begin{pmatrix} j_A & j_A & K \\ -\Omega_A & \Omega_A' & (\tilde{q}-\tilde{q}') \end{pmatrix} (-1)^{2J_i} W(v_i,J_i) \\
&\times \langle \Psi^{\mathrm{el}}_{\bar{n}\Omega_R} \chi^J_{\bar{n}\Omega_R,n\Omega_k}(R) | d_q | \Psi^{\mathrm{el}}_{\Omega_i} \chi^{J_i}_{\Omega_i}(R) \rangle^* \\
&\times \langle \Psi^{\mathrm{el}}_{\bar{n}'\Omega_R'} \chi^J_{\bar{n}'\Omega_R',n'\Omega_k'}(R) | d_{q'} | \Psi^{\mathrm{el}}_{\Omega_i} \chi^{J_i}_{\Omega_i}(R) \rangle, \qquad (9)
\end{aligned}
$$

where the term in the parentheses is a $3j$ symbol.

The indices $\tilde{q}$ and $\tilde{q}'$ in Eq. (9) are defined as $\tilde{q}=\Omega_k-\Omega_i$ and $\tilde{q}'=\Omega_k'-\Omega_i$. In the first order by the Coriolis interaction these indices are limited to the values $\tilde{q}$, $\tilde{q}'=0,\pm1,\pm2$. If only the radial nonadiabatic interactions are important, $\Omega_k=\Omega_R$, $\Omega_k'=\Omega_R'$, $q=\tilde{q}$, $q'=\tilde{q}'$, and the generalized dynamical function $f_K(q,q',q,q')$ in Eq. (9) becomes equivalent to the dynamical function $f_K(q,q')$.[10]

The dynamical functions $f_K(q,q',\tilde{q},\tilde{q}')$ obey the following symmetry rules:[3,10]

$$
\begin{aligned}
f_K(-q,-q',-\tilde{q},-\tilde{q}') &= (-1)^K f_K(q,q',\tilde{q},\tilde{q}'), \\
f_K(q',q,\tilde{q}',\tilde{q}) &= (-1)^{\tilde{q}-\tilde{q}'} f_K^*(q,q',\tilde{q},\tilde{q}').
\end{aligned} \qquad (10)
$$

Instead of the polarization cross section $\sigma^{(j_A)}_{KQ}(\theta,\phi)$ in Eq. (1) it is convenient to use the atomic state multipole moments $\rho^{(j_A)}_{KQ}(\theta,\phi)$ defined as

$$
\rho^{(j_A)}_{KQ}(\theta,\phi) = \frac{\sigma^{(j_A)}_{KQ}(\theta,\phi)}{(2j_A+1)^{1/2}\sigma_0}. \qquad (11)
$$

Later we will skip the upper index (j_A) in Eq. (11) for brevity. In the next section Eqs. (1), (2), and (7) will be used for the analysis of several important particular cases of the recoil distribution of the fragment state multipole moments of the ranks $K=0$, 1, and 2.

III. ANALYSIS OF THE RANK $K=0,1,2$ ANGULAR MOMENTUM DISTRIBUTIONS

A. $K=0$

If the photofragment rank K is equal to zero, Eq. (1) describes the differential cross section for the photofragments A flying apart in the direction specified by the polar angles θ, ϕ. The corresponding angular distribution is well known. In particular, if the photolysis light is linearly polarized, the differential cross section can be written as[8]

$$
\sigma_{00}(\hat{\mathbf{k}}) = \frac{\sigma_0}{4\pi}[1+\beta P_2(\cos\Theta)], \qquad (12)
$$

where Θ is the angle between the light polarization vector $\mathbf{e}$ and the recoil vector $\hat{\mathbf{k}}$.

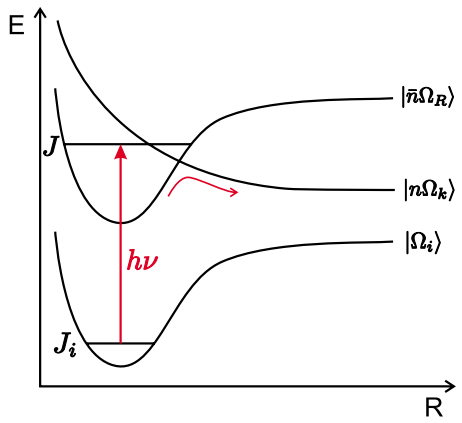

FIG. 1. (Color online) Schematic diagram of the potential curves of a diatomic molecule relevant to the predissociation process.

Assuming that the photolysis proceeds via a single dissociative state $|\Omega_k\rangle$ and using Eqs. (2) and (3), the anisotropy parameter β in Eq. (12) can be presented in the following compact form:

$$
\beta = \sqrt{30}(-1)^{J+J_i}\sqrt{2J+1}\begin{Bmatrix} J & J & 2 \\ 1 & 1 & J_i \end{Bmatrix} C^{J\Omega_k}_{J\Omega_k 20}, \qquad (13)
$$

which is valid for any integer or half-integer values of the angular momenta J_i and J.

The parameter β in Eq. (13) depends on the total angular momenta J_i, J and on the projection Ω_k of J onto the direction of the recoil vector $\hat{\mathbf{k}}$ but not on the other helicity projections Ω_i and Ω_R. Note that the projection Ω_k is always a good quantum number in the asymptotic $R\to\infty$ region and the quantum numbers J and J_i are in general preserved for any molecule. Therefore, Eq. (13) is valid for slow predissociation of any diatomic or polyatomic molecule and for any type of nonadiabatic interaction (radial, Coriolis) involved in the reaction.

For Q, P, and R rotational branches the parameter β in Eq. (13) can be written using the algebraic expressions for the Clebsch–Gordan coefficients and $6j$ symbols[6]

$$
\beta(Q) = -\left[\frac{J_i(J_i+1)-3\Omega_k^2}{J_i(J_i+1)}\right] \quad [Q \ \text{branch}(J=J_i)], \qquad (14)
$$

$$
\beta(Q) = \left[\frac{J_i(J_i+1)-3\Omega_k^2}{J_i(2J_i+1)}\right] \quad [P \ \text{branch}(J=J_i-1)], \qquad (15)
$$

$$
\beta(R) = \left[\frac{(J_i+1)(J_i+2)-3\Omega_k^2}{(J_i+1)(2J_i+1)}\right] \quad [R \ \text{branch}(J=J_i+1)]. \qquad (16)
$$

Equations (13)–(15) generalize previous results reported by Zare,[12] Liyanage and Gordon,[13] and Kuznetsov and Vasyutinskii[2] to the case when the Coriolis interactions can be important. In the absence of the Coriolis interactions, the quantum number Ω_k in Eqs. (13)–(16) is equal to the quantum number Ω_R, which is the projection of the total angular momentum J onto the internuclear distance in the predissociative state, see Fig. 1. In this case, Eqs. (14)–(16) are

equivalent to Eqs. (18)–(20) in Ref. 2 where only radial nonadiabatic interactions have been taken into account.

As follows from Eqs. (13)–(16), in the high-J limit the parameter β does not depend on the quantum numbers J_j, J, and Ω_k and has the following asymptotic values: $\beta(Q)=-1$, $\beta(P)=\beta(R)=1/2$, in agreement with all previous results.[2,12,13]

B. $K=1$

If the photofragment rank K is equal to unity, the state multipole moments in Eqs. (1) and (7) describe the recoil angle distribution of the $Q=0,\pm 1$ components of the fragment orientation[7,8] in the high-J limit. As known,[9,10] in case of direct photodissociation the photofragment orientation can in general be produced by three independent photolysis mechanisms labeled by the anisotropy parameters α_1, γ_1, and γ_1'. When the Coriolis interaction is not included, $\Omega_R=\Omega_k$ (see Fig. 1) and these mechanisms can be characterized by various incoherent/coherent optical excitations of the *predissociative* states Ω_R, Ω_R' in the parent molecule.

When the Coriolis interaction is included, the three possible photolysis mechanisms still can be labeled by the anisotropy parameters α_1, γ_1, and γ_1'; however, in this case they cannot be classified in accordance with their "parallel" or "perpendicular" optical excitation character. Instead, they are classified in accordance with the rank of the light polarization matrix k_d and the coherent quantum number $q_k=\Omega_k-\Omega_k'$ which describes the coherent superposition of the *dissociative* states Ω_k, Ω_k',[3] see Fig. 1. In particular, the parameter α_1 is related to $k_d=1$, $q_k=0$, the parameter γ_1 is related to $k_d=1$, $q_k=\pm 1$, and the parameter γ_1' is related to $k_d=2$, $q_k=\pm 1$. The expressions for each of the three anisotropy parameters in general contain several reaction channels characterized by the radial or Coriolis nonadiabatic interactions and coherent/incoherent optical excitation mechanisms in the parent molecule.[3]

We now analyze the excitation of the P, R, and Q isolated rotational branches on the basis of Eqs. (7) and (9). The first important result of the analysis is that in case of slow predissociation only the mechanism related to the anisotropy parameter γ_1 can produce the photofragment orientation. This predissociation mechanism can be initiated only by the circularly polarized photolysis light.[9]

If the photolysis light is circularly polarized and propagates along the laboratory frame Z axis (geometry III[9]), the angle recoil distributions of the state multipole moments ρ_{10} are given by

$$\rho_{10}(\theta,\phi)=\frac{3\sqrt{3}\sigma\gamma_1(R)}{8\pi(2j_A+1)^{1/2}}\sin^2\theta, \quad R \text{ branch}, \tag{17}$$

$$\rho_{10}(\theta,\phi)=\frac{3\sqrt{3}\sigma\gamma_1(P)}{8\pi(2j_A+1)^{1/2}}\sin^2\theta, \quad P \text{ branch}, \tag{18}$$

$$\rho_{10}(\theta,\phi)=0, \quad Q \text{ branch}, \tag{19}$$

where $\sigma=\pm 1$ for the right and the left circularly polarized light, respectively.

Using Eq. (7) and Table III from Ref. 3, the expressions for the anisotropy parameters $\gamma_1(R)$ and $\gamma_1(P)$ in Eqs. (17) and (18) can be presented in terms of the generalized dynamical functions as

$$\gamma_1(R)=\frac{1}{\mathcal{N}_R}[-b_1+b_2], \tag{20}$$

$$\gamma_1(P)=\frac{1}{\mathcal{N}_P}[b_1+b_2], \tag{21}$$

where

$$b_1=\frac{1}{\sqrt{2}}[2\,\mathrm{Re}\,f_1(0,0,0,1)+\mathrm{Re}\,f_1(1,1,1,2)+\mathrm{Re}\,f_1(1,1,0,1)-\mathrm{Re}\,f_1(1,-1,0,-1)], \tag{22}$$

$$b_2=[\mathrm{Re}\,f_1(1,0,1,0)+\mathrm{Re}\,f_1(1,0,2,1)+\mathrm{Re}\,f_1(1,0,0,-1)-\mathrm{Re}\,f_1(1,0,0,1)]. \tag{23}$$

The predissociation dynamical functions of rank $K=1$ $f_1(q,q',\tilde{q},\tilde{q}')$ in Eqs. (22) and (23) are defined in Eq. (9). The normalization factors $\mathcal{N}_R$, $\mathcal{N}_P$ in Eqs. (20) and (21) are given by

$$\mathcal{N}_R=b_3+b_4, \tag{24}$$

$$\mathcal{N}_P=b_3-b_4, \tag{25}$$

where

$$b_3=f_0(0,0,0,0)+f_0(1,1,1,1)+2f_0(0,0,1,1)+f_0(1,1,2,2)+f_0(1,1,0,0)+f_0(1,-1,0,0), \tag{26}$$

$$b_4=2\sqrt{2}(\mathrm{Re}\,f_0(1,0,0,0)+\mathrm{Re}\,f_0(1,0,1,1)). \tag{27}$$

The normalization factor $\mathcal{N}_Q$ which will be used in section C is given by

$$\mathcal{N}_Q=2[f_0(1,1,1,1)+f_0(1,1,2,2)+f_0(1,1,0,0)-f_0(1,-1,0,0)]. \tag{28}$$

Equations (17)–(27) describe the photofragment state multipole ρ_{10} distributions in slow predissociation of isolated rotational states taking into account the nonadiabatic radial and Coriolis interactions. Each generalized dynamical function in Eqs. (22), (23), (26), and (27) gives contribution from a certain photolysis mechanism resulting in the photofragment orientation, see Tables I and II. Only the dynamical functions $f_1(1,0,1,0)$, $f_0(1,1,1,1)$, $f_0(0,0,0,0)$ in Eqs. (23) and (26) correspond to the cases of pure radial nonadiabatic interactions or no nonadiabatic interactions at all. In particular, the rank $K=1$ dynamical function $f_1(1,0,1,0)=f_1(1,0)$ describes coherent optical excitation of a parallel and a perpendicular transition followed by the radial nonadiabatic transition. The rank $K=0$ dynamical functions $f_0(1,1,1,1)=f_0(1,1)$, $f_0(0,0,0,0)=f_0(0,0)$ describe incoherent parallel and perpendicular optical excitations followed by the radial nonadiabatic transition. In case if the Coriolis interactions are not important Eqs. (22), (23), (26), and (27)

TABLE I. Interpretation of the rank $K=0$ generalized dynamical functions $f_0(q,q',\tilde{q},\tilde{q}')$.

Generalized dynamical function	Possible photolysis scheme
$f_0(0,0,0,0)$	$\Sigma\rightarrow\Sigma\rightarrow\Sigma$
$f_0(1,1,1,1)$	$\Sigma\rightarrow\Pi\rightarrow\Pi$
$f_0(0,0,1,1)$	$\Sigma\rightarrow\Sigma\rightarrow\Pi$
$f_0(1,1,0,0)$	$\Sigma\rightarrow\Pi\rightarrow\Sigma$
$f_0(1,1,2,2)$	$\Sigma\rightarrow\Pi\rightarrow\Delta$
$f_0(1,-1,0,0)$	$\Sigma\rightarrow\Pi_{\pm1}\rightarrow\Sigma$
$f_0(1,0,0,0)$	$\Omega_i=-1/2\rightarrow\Omega_R=\pm1/2\rightarrow\Omega_k=-1/2$
$f_0(1,0,1,1)$	$\Omega_i=-1/2\rightarrow\Omega_R=\pm1/2\rightarrow\Omega_k=1/2$

are equivalent to the expressions reported elsewhere,[2] where the parameter $\tilde{\gamma}_1$ is equal to the parameter γ_1 in Eqs. (17) and (18).

All other generalized dynamical functions in Eqs. (22), (23), (26), and (27) describe the photodissociation mechanisms involving the Coriolis interactions. The physical meanings of the possible photolysis mechanisms are illustrated in Tables I and II and in Figs. 1–4 in Ref. 3. It is interesting to point out that the photofragment orientations in the P and R rotational branches in Eqs. (17)–(27) have the same value in case of the radial nonadiabatic interactions but may differ from each other in case of the Coriolis interactions.

As can be shown by comparing Eqs. (17) and (18) with the results reported elsewhere,[2,3,9] the angular distributions of the photofragment orientation are the same for any photodissociation mechanism. However, the particular anisotropy parameter expressions depend on the photodissociation mechanism.

As shown in Ref. 2 for the slow predissociation via a single excited state $|n_R,\Omega_R\rangle$ mediated by the radial nonadiabatic transition, the orientation dynamical function $f_1(1,0)$ can differ from zero for a diatomic molecule only in the case of $|\Omega_i|=1/2\rightarrow|\Omega_R|=1/2$ transition and if at least one of the states involved is a mixture of the $^2\Sigma_{1/2}$ and $^2\Pi_{1/2}$ states. As can be seen from Eqs. (22) and (23), when the Coriolis transitions are involved to the photolysis, the above restrictions are not valid. In particular, the generalized dynamical functions $f_1(0,0,0,1)$, $f_1(1,1,1,2)$, and $f_1(1,1,0,1)$ in Eq. (22) describe the photolysis schemes $^1\Sigma\rightarrow{}^1\Sigma\rightarrow({}^1\Sigma,{}^1\Pi)$, $^1\Sigma\rightarrow{}^1\Pi\rightarrow({}^1\Pi,{}^1\Delta)$, and $^1\Sigma\rightarrow{}^1\Pi\rightarrow({}^1\Sigma,{}^1\Pi)$, respectively, which all begin from incoherent optical excitation of the ground $^1\Sigma$ state to a single predissociative state continued by a radial and a Coriolis nonadiabatic transition to the coherent $|\Delta\Omega_k|=1$ superposition of the dissociative states. Another photolysis scheme is described by the dynamical function $f_1(1,-1,0,-1)$ in Eq. (22): $^1\Sigma\rightarrow({}^1\Pi_{\pm1})\rightarrow({}^1\Sigma,{}^1\Pi)$. This scheme begins from coherent $|\Delta\Omega|=2$ optical excitation of the ground $^1\Sigma$ state to the predissociative $^1\Pi$ state and is continued by a Coriolis and a radial nonadiabatic transition to the coherent $|\Delta\Omega_k|=1$ superposition of the dissociative states. Therefore, when the Coriolis interaction is not small, the state multipole moments ρ_{10} for the R, P rotational branches can differ from zero also for the $^1\Sigma$ ground state.

TABLE II. Interpretation of the rank $K=1$ generalized dynamical functions $f_1(q,q',\tilde{q},\tilde{q}')$. Only excitation to a single predissociative state $|\Omega_R\rangle$ is considered. Only the dynamical functions which are relevant to the case of slow predissociation are presented in the table.

Generalized dynamical function	Possible photolysis scheme
$f_1(1,0,1,0)$	$\Omega_i=-1/2\rightarrow\Omega_R=\pm1/2\rightarrow\Omega_k=\pm1/2$
$f_1(0,0,0,1)$	$\Sigma\rightarrow\Sigma\rightarrow(\Sigma,\Pi)$ or $\Pi\rightarrow\Pi\rightarrow(\Pi,\Delta)$
$f_1(1,1,1,2)$	$\Sigma\rightarrow\Pi\rightarrow(\Pi,\Delta)$
$f_1(1,1,0,1)$	$\Sigma\rightarrow\Pi\rightarrow(\Sigma,\Pi)$
$f_1(1,-1,0,-1)$	$\Sigma\rightarrow\Pi_{\pm1}\rightarrow(\Sigma,\Pi)$
$f_1(1,0,2,1)$	$\Omega_i=-1/2\rightarrow\Omega_R=\pm1/2\rightarrow\Omega_k=(3/2,1/2)$
$f_1(1,0,0,-1)$	$\Omega_i=-1/2\rightarrow\Omega_R=\pm1/2\rightarrow\Omega_k=(-1/2,-3/2)$
$f_1(1,0,0,1)$	$\Omega_i=-1/2\rightarrow\Omega_R=\pm1/2\rightarrow\Omega_k=\mp1/2$

In the case of the broadband optical excitation of the P, Q, and R rotational branches, the summation over all rotational branches in Eq. (7) should be proceeded. The obtained expressions for the anisotropy coefficients agree with the results reported elsewhere.[3]

C. $K=2$

If the photofragment rank K is equal to 2, the state multipole moments in Eqs. (1) and (7) describe the recoil angle distribution of the $Q=0,\pm1,\pm2$ components of the fragment alignment[7,8] in the high-J limit. As known,[9,10] in case of direct photodissociation the photofragment alignment can in general be produced by five independent photolysis mechanisms labeled by the anisotropy parameters α_2, s_2, γ_2, γ_2', and η_2. When the Coriolis interaction is not included, the parameters α_2 and s_2 are responsible for the incoherent optical excitation of the predissociative states Ω_R via the parallel and perpendicular transitions, the parameters γ_2 and γ_2' are responsible for the $\Delta\Omega_R=\pm1$ coherent optical excitation of a parallel and a perpendicular transition, and the parameter η_2 is responsible for the $\Delta\Omega_R=\pm2$ coherent optical excitation of two perpendicular transitions.

When the Coriolis interaction is included, the possible photolysis mechanisms can in general be labeled by the anisotropy parameters α_2, s_2, γ_2, γ_2', and η_2; however, as discussed above in this case they can be classified in accordance with the rank of the light polarization matrix k_d and the coherent quantum number $q_k=\Omega_k-\Omega_k'$. In particular, the parameter α_2 is related to $k_d=2$, $q_k=0$, the parameter s_2 is related to $k_d=0$, $q_k=0$, the parameter γ_2 is related to $k_d=2$, $q_k=\pm1$, the parameter γ_2' is related to $k_d=1$, $q_k=\pm1$, and the parameter η_2 is related to $k_d=2$, $q_k=\pm2$, see Table III in Ref. 3. The expressions for each of the five anisotropy parameters in general contain several reaction channels characterized by the radial and/or Coriolis nonadiabatic interactions and coherent/incoherent optical excitation mechanisms in the parent molecule.

Using Eqs. (1) and (7) with $K=2$, the expressions for the photofragment state multipole moments ρ_{20}, ρ_{22} produced via excitation of the isolated rotational branches for three basic experimental geometries[9] can be presented in the following forms:

Geometry I: photolysis light is linearly polarized along the Z

TABLE III. Interpretation of the rank $K=2$ generalized dynamical functions $f_2(q,q',\tilde{q},\tilde{q}')$. Only excitation to a single predissociative state $|\Omega_R\rangle$ is considered. Only the dynamical functions which are relevant to the case of slow predissociation are presented in the table.

Generalized dynamical function	Possible photolysis scheme
$f_2(1,1,1,1)$	$\Sigma\rightarrow\Pi\rightarrow\Pi$
$f_2(0,0,0,0)$	$\Sigma\rightarrow\Sigma\rightarrow\Sigma$
$f_2(1,1,0,0)$	$\Sigma\rightarrow\Pi\rightarrow\Sigma$
$f_2(1,1,2,2)$	$\Sigma\rightarrow\Pi\rightarrow\Delta$
$f_2(0,0,1,1)$	$\Sigma\rightarrow\Sigma\rightarrow\Pi$
$f_2(1,-1,0,0)$	$\Sigma\rightarrow(\Pi_{\pm1})\rightarrow\Sigma$
$f_2(1,0,1,1)$	$\Omega_i=-1/2\rightarrow\Omega_R=\pm1/2\rightarrow\Omega_k=+1/2$
$f_2(1,0,0,0)$	$\Omega_i=-1/2\rightarrow\Omega_R=\pm1/2\rightarrow\Omega_k=-1/2$
$f_2(1,0,1,0)$	$\Omega_i=-1/2\rightarrow\Omega_R=\pm1/2\rightarrow\Omega_k=\pm1/2$
$f_2(0,0,0,1)$	$\Sigma\rightarrow\Sigma\rightarrow(\Sigma,\Pi)$
$f_2(1,1,0,1)$	$\Sigma\rightarrow\Pi\rightarrow(\Sigma,\Pi)$
$f_2(1,-1,0,-1)$	$\Sigma\rightarrow\Pi_{\pm1}\rightarrow(\Sigma,\Pi)$
$f_2(1,1,1,2)$	$\Sigma\rightarrow\Pi\rightarrow(\Pi,\Delta)$
$f_2(1,0,2,1)$	$\Omega_i=-1/2\rightarrow\Omega_R=\pm1/2\rightarrow(\Omega_k=3/2,\Omega_k=1/2)$
$f_2(1,0,0,1)$	$\Omega_i=-1/2\rightarrow\Omega_R=\pm1/2\rightarrow(\Omega_k=-1/2,\Omega_k=1/2)$
$f_2(1,0,0,-1)$	$\Omega_i=-1/2\rightarrow\Omega_R=\pm1/2\rightarrow(\Omega_k=-1/2,\Omega_k=-3/2)$
$f_2(1,-1,1,-1)$	$\Sigma\rightarrow(\Pi_{\pm1})\rightarrow(\Pi_{\pm1})$
$f_2(1,-1,2,0)$	$\Sigma\rightarrow(\Pi_{\pm1})\rightarrow(\Delta,\Sigma)$
$f_2(1,1,2,0)$	$\Sigma\rightarrow\Pi\rightarrow(\Delta,\Sigma)$
$f_2(0,0,1,-1)$	$\Sigma\rightarrow\Sigma\rightarrow(\Pi_{\pm1})$
$f_2(1,0,2,0)$	$\Omega_i=-1/2\rightarrow\Omega_R=\pm1/2\rightarrow(\Omega_k=3/2,\Omega_k=-1/2)$
$f_2(1,0,1,-1)$	$\Omega_i=-1/2\rightarrow\Omega_R=\pm1/2\rightarrow(\Omega_k=1/2,\Omega_k=-3/2)$

axis of the laboratory frame.

Q branch ($J=J_i$):

$$\rho_{20}(\theta,\phi)=\frac{\sqrt{5}V_2(j_A)}{4\pi(2j_A+1)^{1/2}}\left\{[P_2(\cos\theta)-[P_2(\cos\theta)]^2]s_2(Q)-\frac{3\eta_2(Q)}{4}\sin^4\theta\right\},\tag{29}$$

$$\rho_{22}(\theta,\phi)=\frac{\sqrt{15}V_2(j_A)}{2\sqrt{2}(2j_A+1)^{1/2}}\frac{1}{4\pi}e^{2i\phi}\times\sin^2\theta\left\{[1-P_2(\cos\theta)]s_2(Q)-\frac{\eta_2(Q)}{2}(1+\cos^2\theta)\right\}.\tag{30}$$

R branch ($J=J_i+1$):

$$\rho_{20}(\theta,\phi)=\frac{\sqrt{5}V_2(j_A)}{4\pi(2j_A+1)^{1/2}}\left\{\left[P_2(\cos\theta)+\frac{1}{2}[P_2(\cos\theta)]^2\right]s_2(R)-\frac{3\eta_2(R)}{4}\sin^4\theta\right\},\tag{31}$$

$$\rho_{22}(\theta,\phi)=\frac{\sqrt{15}V_2(j_A)}{8\pi\sqrt{2}(2j_A+1)^{1/2}}e^{2i\phi}\times\sin^2\theta\left\{\left(1+\frac{1}{2}P_2(\cos\theta)\right)s_2(R)-\frac{\eta_2(R)}{2}(1+\cos^2\theta)\right\}.\tag{32}$$

Geometry II: photolysis light is linearly polarized along the Y axis of the laboratory frame.

Q branch ($J=J_i$):

$$\rho_{20}(\theta,\phi)=\frac{\sqrt{5}V_2(j_A)}{4\pi(2j_A+1)^{1/2}}\left\{P_2(\cos\theta)\left[1+\frac{1}{2}[P_2(\cos\theta)\times(1-\cos2\phi)+\cos2\phi]\right]s_2(Q)+\frac{3}{8}\eta_2(Q)\sin^2\theta(\sin^2\theta+(1+\cos^2\theta)\cos2\phi)\right\},\tag{33}$$

$$\rho_{22}(\theta,\phi)=\frac{\sqrt{15}V_2(j_A)e^{2i\phi}}{8\pi\sqrt{2}(2j_A+1)^{1/2}}\left\{\sin^2\theta\left[1+\frac{1}{2}[P_2(\cos\theta)\times(1-\cos2\phi)+\cos2\phi]\right]s_2(Q)+\frac{\eta_2(Q)}{4}[\sin^2\theta(1+\cos^2\theta)+(1+\cos^2\theta)^2\cos2\phi-4i\cos^2\theta\sin2\phi]\right\}.\tag{34}$$

R branch ($J=J_i+1$):

$$\rho_{20}(\theta,\phi)=\frac{\sqrt{5}V_2(j_A)}{4\pi(2j_A+1)^{1/2}}\left\{P_2(\cos\theta)\left[1-\frac{1}{4}[P_2(\cos\theta)\times(1-\cos2\phi)+\cos2\phi]\right]s_2(R)+\frac{3\eta_2(R)}{8}\sin^2\theta(\sin^2\theta+(1+\cos^2\theta)\cos2\phi)\right\},\tag{35}$$

$$\rho_{22}(\theta,\phi)=\frac{\sqrt{15}V_2(j_A)e^{2i\phi}}{8\pi\sqrt{2}(2j_A+1)^{1/2}}\Bigg\{\sin^2\theta\Bigg[1-\frac{1}{4}[P_2(\cos\theta)\times(1-\cos 2\phi)+\cos 2\phi\Bigg]\Bigg]s_2(R)+\frac{\eta_2(R)}{4}[\sin^2\theta(1+\cos^2\theta)+(1+\cos^2\theta)^2\cos 2\phi-4i\cos^2\theta\sin 2\phi]. \tag{36}$$

Geometry III: photolysis light is circularly polarized and propagates along the Z axis of the laboratory frame. Q branch ($J=J_i$):

$$\rho_{20}(\theta,\phi)=\frac{\sqrt{5}V_2(j_A)}{4\pi(2j_A+1)^{1/2}}\Bigg\{\Bigg[P_2(\cos\theta)+\frac{1}{2}(P_2(\cos\theta))^2\Bigg]s_2(Q)+\frac{3\eta_2(Q)}{8}\sin^4\theta\Bigg\}, \tag{37}$$

$$\rho_{22}(\theta,\phi)=\frac{\sqrt{15}V_2(j_A)e^{2i\phi}\sin^2\theta}{8\pi\sqrt{2}(2j_A+1)^{1/2}}\times\Bigg\{\Bigg(1+\frac{1}{2}P_2(\cos\theta)\Bigg)s_2(Q)+\frac{\eta_2(Q)}{4}(1+\cos^2\theta)\Bigg\}. \tag{38}$$

R branch ($J=J_i+1$):

$$\rho_{20}(\theta,\phi)=\frac{\sqrt{5}V_2(j_A)}{4\pi(2j_A+1)^{1/2}}\Bigg\{\Bigg[P_2(\cos\theta)-\frac{1}{4}(P_2(\cos\theta))^2\Bigg]s_2(R)+\frac{3}{8}\sin^4\theta\eta_2(R)\Bigg\}, \tag{39}$$

$$\rho_{22}(\theta,\phi)=\frac{\sqrt{15}V_2(j_A)e^{2i\phi}}{8\pi\sqrt{2}(2j_A+1)^{1/2}}\times\sin^2\theta\Bigg\{\Bigg(1-\frac{1}{4}P_2(\cos\theta)\Bigg)s_2(R)+\frac{\eta_2(R)}{4}(1+\cos^2\theta)-i\sigma\gamma_2'(R)\Bigg\}. \tag{40}$$

The expressions for the rotational P branch ($J=J_i-1$) can be readily obtained from R-branch expressions in Eqs. (31), (32), (35), (36), (39), and (40) by replacing $s_2(R)\rightarrow s_2(P)$, $\eta_2(R)\rightarrow\eta_2(P)$, and $\gamma_2'(R)\rightarrow\gamma_2'(P)$ given in Eqs. (42), (43), (47), (48), (51), and (52).

The anisotropy parameters s_2, η_2, γ_2' in Eqs. (29)–(40) can be defined as

$$s_2(Q)=\frac{2V_2^{-1}(j_A)}{\mathcal{N}_Q}[f_2(1,1,1,1)+f_2(1,1,2,2)+f_2(1,1,0,0)-\mathrm{Re}\,f_2(1,-1,0,0)], \tag{41}$$

$$s_2(R)=\frac{V_2^{-1}(j_A)}{\mathcal{N}_R}[b_5+b_6], \tag{42}$$

$$s_2(P)=\frac{V_2^{-1}(j_A)}{\mathcal{N}_P}[b_5-b_6], \tag{43}$$

where

$$b_5=f_2(1,1,1,1)+f_2(0,0,0,0)+2f_2(0,0,1,1)+f_2(1,1,2,2)+f_2(1,1,0,0)+\mathrm{Re}\,f_2(1,-1,0,0), \tag{44}$$

$$b_6=2\sqrt{2}(\mathrm{Re}\,f_2(1,0,1,1)+\mathrm{Re}\,f_2(1,0,0,0)), \tag{45}$$

$$\eta_2(Q)=\frac{\sqrt{6}V_2^{-1}(j_A)}{2\mathcal{N}_Q}[f_2(1,-1,1,-1)+2\,\mathrm{Re}\,f_2(1,-1,2,0)-2\,\mathrm{Re}\,f_2(1,1,2,0)], \tag{46}$$

$$\eta_2(R)=\frac{\sqrt{6}V_2^{-1}(j_A)}{8\mathcal{N}_R}[b_7+b_8], \tag{47}$$

$$\eta_2(P)=\frac{\sqrt{6}V_2^{-1}(j_A)}{8\mathcal{N}_P}[b_7-b_8], \tag{48}$$

where

$$b_7=f_2(1,-1,1,-1)+2f_2(0,0,1,-1)+2\,\mathrm{Re}\,f_2(1,1,2,0)+2\,\mathrm{Re}\,f_2(1,-1,2,0), \tag{49}$$

$$b_8=2\sqrt{2}(\mathrm{Re}\,f_2(1,0,2,0)+\mathrm{Re}\,f_2(1,0,1,-1)), \tag{50}$$

$$\gamma_2'(R)=\frac{\sqrt{6}V_2^{-1}(j_A)}{2\mathcal{N}_R}[b_9+b_{10}], \tag{51}$$

$$\gamma_2'(P)=\frac{\sqrt{6}V_2^{-1}(j_A)}{2\mathcal{N}_P}[-b_9+b_{10}], \tag{52}$$

where

$$b_9=2\,\mathrm{Im}\,f_2(0,0,0,1)+\mathrm{Im}\,f_2(1,1,1,2)+\mathrm{Im}\,f_2(1,1,0,1)+\mathrm{Im}\,f_2(1,-1,0,-1), \tag{53}$$

$$b_{10}=\sqrt{2}[\mathrm{Im}\,f_2(1,0,1,0)+\mathrm{Im}\,f_2(1,0,2,1)+\mathrm{Im}\,f_2(1,0,0,1)+\mathrm{Im}\,f_2(1,0,0,-1)]. \tag{54}$$

The dynamical functions $f_2(q,q',\tilde{q},\tilde{q}')$ in Eqs. (41), (44)–(46), (49), (50), (53), and (54) are defined in Eq. (9) and the normalization factors $\mathcal{N}_Q$, $\mathcal{N}_R$, and $\mathcal{N}_P$ are given in Eqs. (28), (24), and (25), respectively. The factor $V_2(j_A)$ is given by

$$V_2(j_A) = 5\left[\frac{j_A(j_A+1)}{(2j_A+3)(2j_A-1)}\right]^{1/2}. \quad (55)$$

In the absence of the Coriolis interactions, the parameters $s_2(Q)$, $s_2(R)$, $s_2(P)$, $\eta_2(Q)$, $\eta_2(R)$, $\eta_2(P)$, $\gamma_2'(R)$, and $\gamma_2'(P)$ in Eqs. (41)–(43), (46)–(48), (51), and (52) are related to the corresponding anisotropy parameters $s_2^{(0)}$, $\tilde{s}_2$, $\eta_2^{(0)}$, $\tilde{\gamma}_2'$ in Ref. 2 as follows: $s_2(Q)=s_2^{(0)}$, $s_2(R)=s_2(P)=\tilde{s}_2$, $\eta_2(Q)=\frac{1}{2}\eta_2^{(0)}$, $\eta_2(R)=\eta_2(P)=\frac{1}{4}\eta_2^{(0)}$, $\gamma_2'(R)=\gamma_2'(P)=\tilde{\gamma}_2'$.

Equations (29)–(54) describe the laboratory frame multipole moments ρ_{20}, ρ_{22} in the slow predissociation of a single rotational state where both radial and Coriolis nonadiabatic interactions are taken into account. As can be seen from Eqs. (29)–(40), in the case of slow predissociation the total number of the anisotropy parameters needed for description of the photofragment alignment is reduced to 3.

The multipole moment recoil angle distributions in the case of slow predissociation in Eqs. (29)–(40) can be formally obtained from those in the case of direct photodissociation tabulated by Wouters *et al.*[9] by holding the parameter γ_2 equal to zero and by assigning the relationship $2\alpha_2=s_2$ if the Q rotational branch is excited and $4\alpha_2=-s_2$ if R or P rotational branch is excited. However, the expressions for the anisotropy parameters in terms of the dynamical functions in these two cases are different.

Only the dynamical functions $f_2(1,1,1,1)=f_2(1,1)$, $f_2(0,0,0,0)=f_2(0,0)$, $f_2(1,-1,1,-1)=f_2(1,-1)$, and $f_2(1,0,1,0)=f_2(1,0)$ in Eqs. (41)–(54) describe the radial nonadiabatic interactions. All other dynamical functions contain contributions from the Coriolis interactions. Each generalized dynamical function in Eqs. (41)–(54) is related to a certain photolysis mechanism resulting in the photofragment alignment; the examples are given in Table III.

As can be seen from Eqs. (42)–(45) and (47)–(54), in the absence of the Coriolis interactions the alignment parameters $s_2(R)$ and $s_2(P)$, $\eta_2(R)$ and $\eta_2(P)$, $\gamma_2'(R)$ and $\gamma_2'(P)$ which are referred to the R and P rotational branches have the same values in pairs. However, if the Coriolis interaction is included, these parameters may differ from each other.

The multipole moments defined above refer to the laboratory frame. The transformation to the frequently used molecular frame multipole moments $\rho_{2q_k}^{\mathrm{mol}}$ which are defined with respect to the photofragment recoil vector $\hat{\mathbf{k}}$ can be obtained using the transformation[10]

$$\rho_{2Q}(\theta,\phi) = (2j_A+1)^{1/2}\rho_{00}(\theta,\phi)\sum_{q_k} D^{2*}_{Qq_k}(\phi,\theta,0)\rho^{\mathrm{mol}}_{2q_k}, \quad (56)$$

where the projection $q_k=\Omega_k-\Omega_k'=\Omega_A-\Omega_A'$ is limited to the values $q_k=0,\pm1,\pm2$.

Equation (56) differs from the conventional irreducible tensor transformation under rotation of the coordinate frame[6] by an additional factor $(2j_A+1)^{1/2}\rho_{00}(\theta,\phi)$ in the right hand side. The factor appears because the laboratory frame multipole moment $\rho_{2Q}(\theta,\phi)$ in the left hand side of Eq. (56) is normalized to the total number of the photofragments integrated over all recoil angles, while the molecular frame multipole moment $\rho_{2q_k}^{\mathrm{mol}}$ in the right hand side of Eq. (56) is normalized to the number of the photofragments moving in the direction $\hat{\mathbf{k}}(\theta,\phi)$.

When the photolysis light is linearly polarized along the laboratory Z axis, explicit expressions for the molecular frame multipole moments can be readily obtained by comparing Eqs. (29)–(32) with Eq. (56) and presented in the form

$$\rho_{20}^{\mathrm{mol}} = \frac{\sqrt{5}V_2(j_A)s_2(i)}{(2j_A+1)^{1/2}} \quad \text{where}$$
$$i=P,Q,R \quad (P,Q,R \text{ branches}), \quad (57)$$

$$\rho_{21}^{\mathrm{mol}} = 0 \quad (P,Q,R \text{ branches}), \quad (58)$$

$$\rho_{22}^{\mathrm{mol}} = -\sqrt{\frac{5}{6}}\frac{V_2(j_A)\eta_2(Q)}{(2j_A+1)^{1/2}} \quad (Q \text{ branch}), \quad (59)$$

$$\rho_{22}^{\mathrm{mol}} = -\sqrt{\frac{10}{3}}\frac{V_2(j_A)\eta_2(l)}{(2j_A+1)^{1/2}}\frac{\sin^2\theta}{1+\cos^2\theta} \quad \text{where}$$
$$l=P,R \quad (P,R \text{ branches}). \quad (60)$$

The molecular frame multipole moment ρ_{20}^{mol} refers to the diagonal matrix elements of the photofragment density matrix $\rho_{\Omega_A\Omega_A}$ and the multipole moment $\rho_{22}^{\mathrm{mol}}=\rho_{2-2}^{\mathrm{mol}}$ refers to the off-diagonal matrix elements of the photofragment density matrix $\rho_{\Omega_A\Omega_A'}$, where $\Omega_A-\Omega_A'=2$. In the absence of the Coriolis interaction multipole moment ρ_{20}^{mol} is produced by the incoherent $\Omega_R=\Omega_R'$ optical excitation of the parent molecule and the multipole moment ρ_{22}^{mol} is produced by the coherent $\Omega_R-\Omega_R'=2$ optical excitation of the parent molecule.

As shown in Eqs. (57)–(60), the multipole moments ρ_{20}^{mol} for all P, Q, and R rotational branches and the multipole moment ρ_{22}^{mol} for the Q rotational branch in the high-J limit do not depend on the angle θ between the light polarization $\mathbf{e}$ and the recoil direction $\hat{\mathbf{k}}$. However, the multipole moment ρ_{22}^{mol} for the P and R rotational branches does depend on the angle θ.

For the moment, only a few experimental works have been carried out in the field of the photofragment alignment produced in slow predissociation of diatomic molecules. Katô and Onomichi[14] and Frohlich *et al.*[15] investigated the polarization of light emitted by photofragments produced in slow predissociation of Cs_2 and H_2, respectively. In both studies the theoretical treatments based on the analysis of the alignment of the photofragment angular momenta averaged over all recoil directions.

Very recently Rose *et al.*[16] reported strong alignment of the $S(^2P_{1,2})$ products in the predissociation of SH and SD radicals via the $X\,^2\Pi \rightarrow A\,^2\Sigma$ optical transition along with a weak sensitivity of the fine-structure branching ratio to excess energy. Analyzing the experimental recoil angle distribution of the photofragments produced and detected by linearly polarized light, Rose *et al.*[16] neglected the effect of coherence between the Ω_k states and determined the photofragment multipole moment ρ_{20}^{mol}, see Eq. (57). They resumed that the experimental data do not fit the predictions of either

adiabatic or diabatic photodissociation, emphasizing the need for a fully quantum treatment. Note that Eqs. (9) and (41)–(43) for the anisotropy parameters in terms of the dynamical functions obtained in the high-J limit cannot be directly applied to the experimental data of Rose *et al.*[16] obtained for very low J values. However, the angular distributions of the multipole moments in Eqs. (29)–(40) hold in general and valid for any J value.

In the case of the broadband excitation of the Q, R, and P rotational branches the summation over all rotational quantum numbers $J=J_i, J_i \pm 1$ should be proceeded in Eq. (7). The resulting expressions for the photofragment state multipole moments coincide with the expressions reported elsewhere.[3] Note that the expressions for the parameters s_2 and η_2 in Ref. 3 contain errors. The dynamical function $f_2(0,0,1,1)$ in Eq. (45) in Ref. 3 should be doubled. Similarly, one should put $2\,\mathrm{Re}\, f_2(1,-1,2,0)$ instead of $f_2(1,-1,2,0)$ in Eq. (49) in Ref. 3.

Equations (12), (17)–(19), and (29)–(40) together with the expressions for the intensity of the 2+1 Resonance Enhanced Multiphoton Ionization (2+1 REMPI) for different probe light polarizations tabulated by Wouters *et al.*[9] provide a theoretical link to the observations of the orbital polarization of products of predissociation and allow for determination of the anisotropy parameters of the ranks $K=0,1,2$ from experiment. As shown above, when the Coriolis interaction is included, the anisotropy parameters become linear combinations of numerous dynamical functions each describing a certain photolysis mechanism. Therefore, it seems unlikely that the dynamical functions can be determined experimentally within the frame of assumed experimental procedure of detection of polarization of one of the reaction product at the asymptotically large interfragment distance R. Possible ways of increasing the number of information obtained from experiment may be using the coincidence detection of polarization of both products and the femtosecond real-time detection technique.

It should be also noted that although the anisotropy parameters/anisotropy transforming coefficients can be defined at any value of the molecular total angular momentum J, the dynamical functions in Eq. (9) can be defined only in the high-J limit. Therefore, in case of small J values general expression for the anisotropy transforming coefficients (2) should be used which can unlikely provide a clear interpretation of different dissociation mechanisms contributing to each coefficient.

IV. CONCLUSION

Quantum mechanical expressions describing the recoil angle dependence of the photofragment state multipoles in the case of slow predissociation of isolated rotational states have been derived on the basis of the theory developed elsewhere[2,3] where both radial and Coriolis nonadiabatic interactions between different PESs have been taken into account.

The state multipole moments with the ranks $K=0$, 1, and 2 describing the photofragment angular distribution and the photofragment angular momentum polarization (orientation and alignment) have been derived and analyzed in detail. As shown, the recoil-angle-dependent part of the state multipole moments in terms of the anisotropy parameters have the same universal form irrespective of the photolysis mechanism. The particular expressions for the anisotropy parameters of the ranks $K=0,1,2$ have been derived. As shown, the total number of the anisotropy parameters of the ranks $K=0,1,2$ which completely describe the predissociation dynamics is equal to 5. These are one zeroth-rank parameter β, one first-rank (orientation) parameter γ_1, and three second-rank (alignment) parameters s_2, γ_2', η_2. The expressions for the anisotropy parameters are presented in terms of the generalized dynamical functions $f_K(q,q',\tilde{q},\tilde{q}')$ each containing contribution from a certain photolysis mechanism including incoherent/coherent optical excitation of the parent molecule followed by the radial and/or Coriolis nonadiabatic transition to the dissociative molecular state.

ACKNOWLEDGMENTS

The authors are much grateful to Professor A. G. Suits for fruitful discussions. The work was supported by the Russian Foundation for Basic Researches, Grant No. 08-03-00601-a and by the US National Science Foundation under Award No. CHE-0715300.

[1] V. V. Kuznetsov and O. S. Vasyutinskii, J. Chem. Phys. **123**, 034307 (2005).
[2] V. V. Kuznetsov and O. S. Vasyutinskii, J. Chem. Phys. **127**, 044308 (2007).
[3] P. S. Shternin and O. S. Vasyutinskii, J. Chem. Phys. **128**, 194314 (2008).
[4] E. E. Nikitin and S. Y. Umanskii, *Theory of Slow Atomic Collisions* (Springer, Berlin, 1984).
[5] H. Lefebvre-Brion and R. W. Field, *Perturbation in the Spectra of Diatomic Molecules* (Academic, New York, 1986).
[6] D. A. Varshalovich, A. N. Moskalev, and V. K. Khersonskii, *Quantum Theory of Angular Momentum* (World Scientific, Singapore, 1988).
[7] K. Blum, *Density Matrix Theory and Applications*, 2nd ed. (Plenum, New York, 1996).
[8] R. N. Zare, *Angular Momentum* (World Scientific, New York, 1988).
[9] E. R. Wouters, M. Ahmed, D. S. Peterka, A. S. Bracker, A. G. Suits, and O. S. Vasyutinskii, *Imaging in Chemical Dynamics* (American Chemical Society, Washington, DC, 2000), p. 238.
[10] A. G. Suits and O. S. Vasyutinskii, Chem. Rev. (Washington, D.C.) **108**, 3706 (2008).
[11] J. A. Beswick and O. S. Vasyutinskii, Comments At. Mol. Phys. **42**, 69 (1998).
[12] R. N. Zare, Ber. Bunsenges. Phys. Chem **86**, 422 (1982).
[13] R. Liyanage and R. J. Gordon, J. Chem. Phys. **107**, 7209 (1997).
[14] H. Katô and K. Onomichi, J. Chem. Phys. **82**, 1642 (1985).
[15] H. Frohlich, M. Glass-Maujean, L. D. A. Siebbeles, and O. S. Vasyutinskii, Z. Phys. D: At., Mol. Clusters **34**, 119 (1995).
[16] R. A. Rose, A. Orr-Ewing, C.-H. Yang, K. Vidma, G. C. Groenenboom, and D. H. Parker, J. Chem. Phys. **130**, 034307 (2009).